DESIGN AND PREPARATION OF ULTRA-THIN CARBON FIBER REINFORCED POLYETHER ETHER KETONE COMPOSITE FOLDABLE HINGES

Zhiyang SONG[1], Mengkai LI[1], Chao QIU[1,*], Lipeng WANG[2], Wenlan BA[1], Shijie ZHU[1], Haihong WU[1]

To overcome the limitations of thermally driven shape memory composites in practical applications, this study prepared carbon fiber reinforced polyether ether ketone (CF/PEEK) shape memory composites and designed the layup of the electrically driven hinge and the conductive layer materials. The infrared thermal imaging changes and temperature distribution uniformity during the heating deployment process of CF/PEEK shape memory composites were analyzed, and the relationship between heating temperature and deformation angle was investigated. The results show that at a heating temperature of 320°C, the electrically driven sheet hinge can achieve 100% shape recovery within a relatively short time of 13 seconds. After the external force was removed, the thermally driven sample exhibited a recovery ratio of only about 10% at 180°C. In comparison, the electrically driven sample demonstrated better stability in shape fixity. Subsequently, the material was applied and validated in electrically driven foldable plates and complex folded structures. The shape memory foldable plate completed deformation and recovery within approximately 31 seconds under the drive of a 6V DC circuit. The electrically driven deformation of the CF/PEEK shape memory composites was achieved through heating via the Joule heating effect.

Keywords: Polyether ether ketone; Carbon fiber thinning; Shape-memory composite material; Thermal stress; Active deformation

1. Introduction

In recent years, electro-driven shape memory polymer composites (SMPCs) have garnered considerable attention due to their broad application potential, including artificial muscles [1], micro-robots [2], bionic devices [3], and deployable aerospace structures [4]. Shape memory polymers (SMPs), as a class of intelligent polymers, can recover their original shape from a pre-deformed configuration when exposed to external stimuli such as light, magnetic fields, solvents, or heat [5–6]. Despite advantages including low density, large recoverable strain, low energy

* Corresponding author, Chao Qiu, e-mail: qiunjcust@126.com
[1] School of Mechanical and Electrical Engineering, Henan University of Technology, Zhengzhou, 450001, China
[2] Xi'an Institute of Space Radio Technology, Xi'an, 710000, China

consumption, and excellent processability, SMPs still suffer from low strength and limited recovery force [7–8]. Moreover, their actuation typically relies on external heat sources, which reduces control precision. To address these limitations, conductive particles and fibers have been incorporated into SMPs to enable electro-driven actuation [9]. Carbon fiber–reinforced SMPCs, in particular, have been widely employed in space-deployable active deformation components such as hinges, truss arms, and morphing structures [10]. However, the actuation of these composites remains irreversible and requires mechanical reshaping under different temperature conditions, a process that is also time-consuming.

Continuous fibers are widely recognized for their combination of low density, high strength, and high electrical and thermal conductivity. Owing to their highly aligned internal structure, these properties can be effectively transferred to the macroscopic scale [11-13]. When a voltage is applied to conductive SMPCs, resistive (Joule) heating is generated, which raises the temperature of the composite and activates the shape memory effect (SME). Compared with direct external heating, Joule heating provides convenient, uniform, and remotely controllable actuation. As a result, electrically triggered SME is well suited for applications in which direct heating is impractical, including self-deployable aerospace structures, implantable biomedical devices, actuators, and sensors [14-16]. Under an applied current, carbon fibers (CFs) can exhibit heating rates of up to 2000 K/ms, indicating a rapid electrothermal response. Because polymers are thermal insulators, localized regions of the SMP can be heated while surrounding areas remain largely unaffected. Spatial control over the location and sequence of shape recovery can therefore be achieved, as recovery occurs only in the locally heated regions. Dai et al. [17] demonstrated controllable spatially electroactive shape recovery in carbon nanotube (CNT)-filled SMPs by selectively applying voltage at specific positions. In their work, the heat generated by the current was precisely controlled, enabling remote and site-specific manipulation of shape recovery within the structure. By locally adjusting the applied voltage in SMPCs, both the stress release rate and the shape recovery rate can be regulated. Over the past five years, substantial effort has been devoted to achieving complex and controllable shape recovery in SMPs [18]. Selective heating of SMPCs has emerged as a concise and efficient strategy for realizing intricate, spatially programmable shape recovery

The most common heating strategy is to expose the material to high-temperature gases or liquids, thereby increasing its ambient temperature (external heating). However, this indirect approach is unsuitable for many practical applications [19]. For example, when SMPs are employed as active deformation structures in aerospace systems, it is not feasible to heat the device by raising the surrounding temperature in outer space. A common alternative is to generate heat internally within the material. Electrical, magnetic, optical, acoustic, and chemical energy can all be converted into thermal energy to realize such internal heating [20].

In this context, the feasibility of electro-driven deformation in CF/PEEK composites is investigated through the design of an electro-driven hinge. The practicality of these materials for active deformation structures is further demonstrated by designing electro-driven folding plates and other complex configurations. The introduction of continuous fiber layers eliminates issues such as nonuniform dispersion of conductive particles in the SMP matrix and the complexity of constructing conductive networks. Special pretreatment of fillers is no longer required, which facilitates uniform dispersion and improves interfacial heat transfer. At the same time, superior mechanical performance is provided.

2. Materials and methods

2.1 Experimental materials

Ultra-thin carbon fiber tape was provided by Zhengzhou Fangxian New Material Technology Co., Ltd. The carbon fiber (12K T700S CF) has a diameter of 7 μm, a thermal expansion coefficient of -0.38×10^{-6} °C^{-1}, a tensile strength of 4900 MPa, and a tensile modulus of 230 GPa. PEEK film was obtained from Victrex (UK) with a thickness of 0.006 mm, a glass transition temperature (Tg) of 143 °C, and a melting temperature of 343 °C. The linear thermal expansion coefficients (α) below and above Tg are 47×10^{-6} °C^{-1} and 120×10^{-6} °C^{-1}, respectively. The film also exhibits a Poisson's ratio of 0.45, a tensile strength of 120 MPa, and an elastic modulus of 2.4 GPa.

2.2 Design and fabrication of lamellar hinges

To ensure process consistency, the lamellar hinges were fabricated using the CF/PEEK molding and curing procedures previously established by the research group. The mold press was heated to 85 °C and held for 5 min, then heated to 135 °C and maintained for 15 min under a molding pressure of 0.1 MPa. The layup consisted of three layers: a 0.006 mm-thick PEEK film as the top layer, a 0.14 mm-thick CF prepreg as the second layer, and Ni–Ti alloy wires with a diameter of 0.05 mm as the third layer. The Ni–Ti wires were spaced at 3 mm intervals. The design and fabrication process of the lamellar hinge is shown in Fig. 1. The lamellar shape memory hinge was produced by hot-press molding, and the final sample dimensions were 15 mm × 15 mm × 0.15 mm.

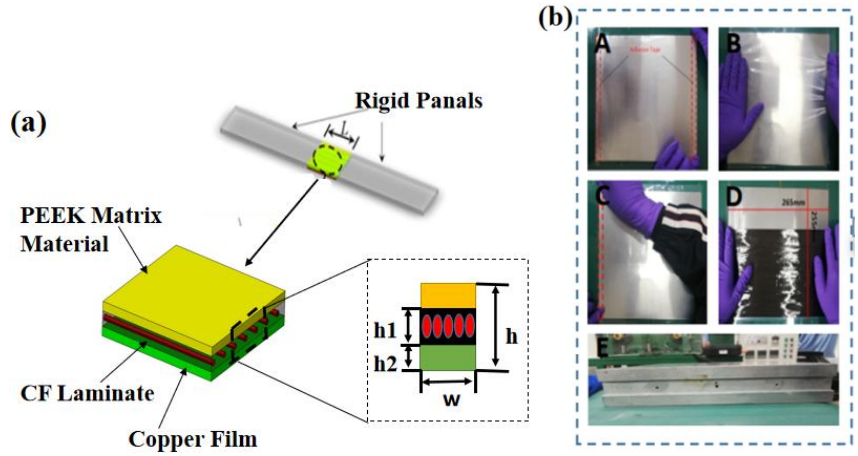

(a) Design schematic diagram (b) Fabrication process diagram

Fig.1 Schematic diagram of the preparation process for the shape memory hinge sheet

2.3 Fabrication of shape memory folding plates

An integrated molding process was employed to design and fabricate shape memory hinge sheets combined with CF/epoxy rigid panels, yielding an ultrathin folding plate with dimensions of 100 mm × 50 mm × 0.15 mm and shape memory functionality. The physical specimen and structural schematic are shown in Fig. 2. The plate consists of two regions: a deformation zone and a non-deformation (rigid) zone. The deformation zone, where the hinges are arranged, comprises four layers—PEEK, CF prepreg, Ni–Ti alloy wires, and copper foil—with overall dimensions of 15 mm × 50 mm × 0.15 mm. The non-deformation rigid zone is formed by curing the CF/epoxy prepreg to the same thickness.

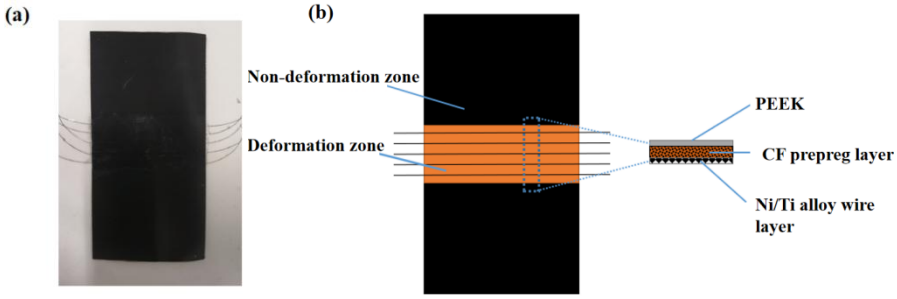

(a) Physical photograph of the folding plate (b) Schematic diagram of the structure

Fig. 2 Physical photograph and structural schematic diagram of the shape memory folding plate

2.4 Shape memory recovery performance testing

2.4.1 Electrically driven behavior

To evaluate the shape memory performance of the electrically driven hinge, the specimen was heated to 240 °C, bent to a 90° angle under an external load, and

held in this configuration until cooling and fixation were completed. After the load was removed, the specimen kept the programmed shape without external constraints. A 6 V DC power supply (MAISENG, MS1520DS) was then used as the driving source and connected to the electrodes reserved at both ends of the specimen. Electrical resistance was measured by connecting both ends of the sample to a DC resistance tester (Jinko JK2512). The specimen was subsequently heated by electrical actuation, and its shape evolution during recovery was recorded and observed.

2.4.2 Thermally driven behavior

To compare the shape recovery rates under electrical and thermal actuation, a hinge pre-bent to 90° was placed on a constant-temperature heating stage. The hinge was heated from 180 °C to 320 °C at a rate of 10 °C/s, and the recovery process of the hinge sheet was recorded

3. Results and analysis

3.1 Shape memory behavior of electrically driven lamellar hinges

To verify the heating capability of the specimen, a 15 mm × 15 mm lamellar hinge was prepared to evaluate its electrothermal actuation performance, as shown in Fig. 3. The resistance of the sample was measured using a multimeter, and the volume resistivity between the two ends of the material was calculated according to Equation (1):

$$\rho = \frac{RA}{L} \tag{1}$$

where R is the measured resistance of the specimen, L is the measured distance between the two electrodes, and A is the cross-sectional area of the specimen.

To avoid poor electrical contact and to enhance heating of the alloy wires, the specimen was clamped with copper sheets before connection to the positive and negative terminals of the power supply. The supply voltage was then incrementally increased in steps of 0.5 V to drive the specimen electrically. The relationship between specimen temperature and heating power during electrothermal tests is shown in Fig. 4. As the applied voltage increased, the specimen temperature rose accordingly. Below 300 °C, this increase was approximately linear. When the temperature exceeded 300 °C, the heating rate decreased slightly because of heat dissipation. At 6 V, corresponding to a heating power of 22 W, the specimen temperature rapidly reached 320 °C within 8 s. During cooling, when the voltage was set to zero, the temperature of the CF conductive layer dropped almost instantaneously, and the specimen surface temperature returned to room temperature within approximately 1–2 s. These results confirm that the heating-layer design provides the desired electrothermal performance.

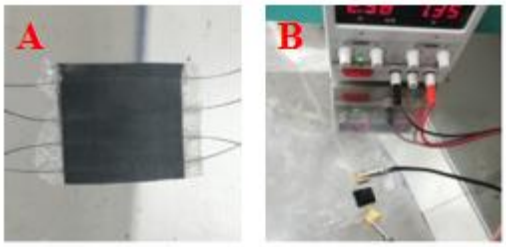

(a) Physical photograph of the specimen (b) Electrothermal driving test
Fig.3 Test of electro-thermal actuation performance for the laminate hinge

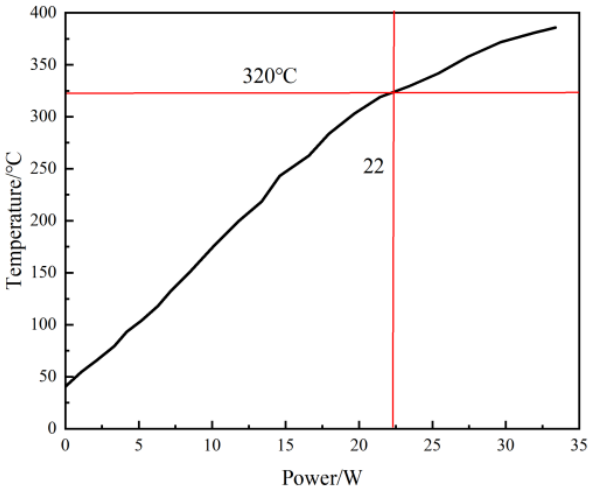

Fig. 4 Relationship between heating power and temperature in the electro-thermal actuation test

The electrically driven shape recovery behavior of the CF/PEEK composite lamellar hinge is shown in Fig. 5. Under an applied voltage of 6 V, nearly complete recovery to the original shape was achieved within 13 s. The recovery rate is primarily governed by the magnitude of the applied voltage and by the amount and spatial distribution of Ni–Ti alloy wires in the specimen. During electrothermal actuation, the temperature distribution was monitored using an infrared camera. Under constant voltage, electrically triggered shape recovery was recorded with an optical camera, and the corresponding infrared thermal images are presented in Fig. 6. After the power supply was connected, the infrared camera was positioned directly above the specimen. Because the hinge was initially in a folded state, the temperature on the right side of the image was higher than that on the left. With continued heating, the hinge gradually unfolded, and a more uniform temperature distribution across the surface was observed. When the specimen temperature reached approximately 320 °C, rapid unfolding occurred, resulting in complete shape recovery. No thermal degradation or interfacial delamination occurred, demonstrating excellent thermal stability of the material itself, which can withstand

electrodriven cycling at this temperature. The relationship between recovery angle and time is shown in Fig. 7. During the initial 0–5 s of heating, angle recovery was slow. As heating proceeded, the temperature increased to about 320 °C within 8 s, leading to a marked acceleration in recovery. A fully flattened state was obtained within 13 s.

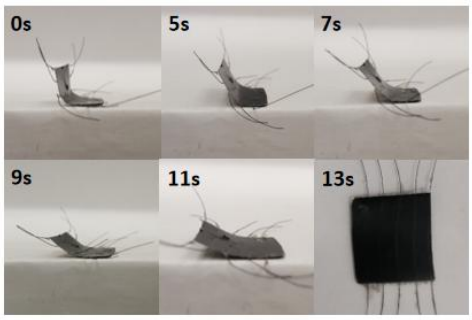

Fig. 5 Shape recovery process of the electrically-driven laminated hinge

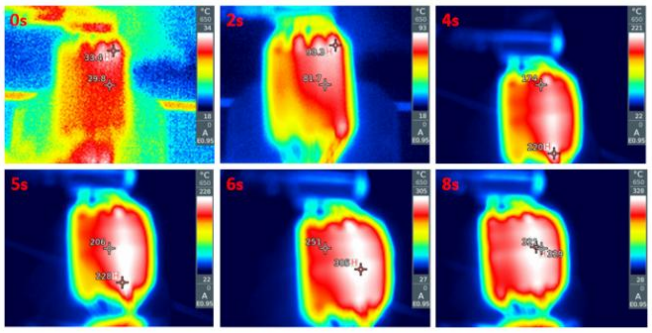

Fig. 6 Infrared thermal imaging of the electrically-driven laminated hinge during heating

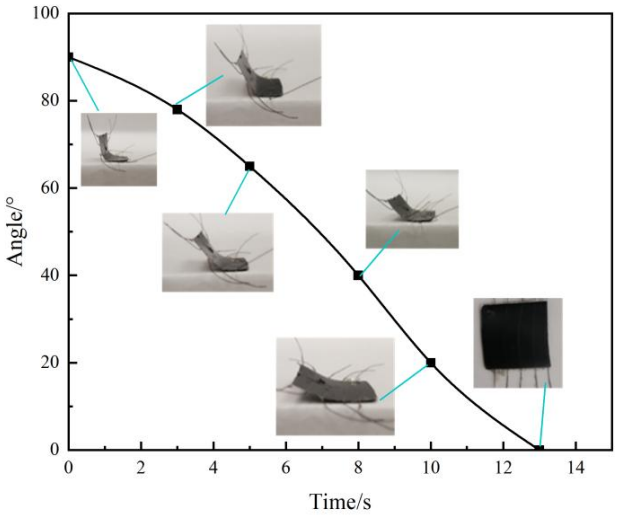

Fig.7 Relationship between the recovery angle and recovery time of the specimen

The shape recovery and fixation rates of the lamellar hinge under different driving modes are presented in Fig. 8. Because electrothermal actuation provides more uniform heating than conventional thermal driving, the recovery rate at a given temperature is slightly higher, and the CF/PEEK composite maintained excellent shape memory performance. Under thermal driving, heating on the hot stage was nonuniform owing to the folded configuration of the specimen. At 180 °C, the recovery ratio was only about 10%. As the temperature increases, the curled structure gradually unfolds and the heated area expands, and full recovery was eventually achieved in approximately 20 s; however, the surface temperature remains nonuniform throughout the unfolding process. In contrast, electrothermal heating yields a more uniform temperature distribution and allows more accurate temperature control. The recovery rate is more stable, and 100% shape recovery was obtained in a shorter time of about 13 s. A similar trend is observed for the fixation rate. With improved temperature control during programming, removal of the external load after heating results in superior shape stability for electrothermally driven specimens, as shown in Fig. 8(b).

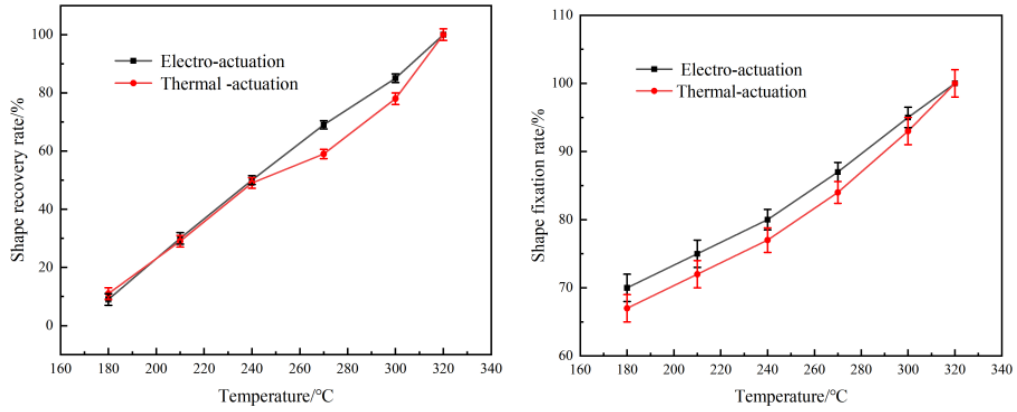

(a) Shape recovery rate (b) Shape fixation rate

Fig. 8 Comparison between electrically-driven and thermally-driven systems

3.2 Behavior of electrically driven shape memory folding plates

The same procedure was used to perform an electrically driven shape memory deformation test on the folding plate. The shape recovery and deformation process is shown in Fig. 9. When a 5 V voltage was applied and the temperature exceeded 180 °C, the softened specimen was folded to 180° under an external load. While the load was maintained, the sample was cooled to room temperature to fix the programmed shape. The constraint was then removed, and an electrically driven recovery test was carried out using a 6 V DC circuit. The specimen exhibited stable

recovery behavior and returned completely to a flat configuration within approximately 31 s.

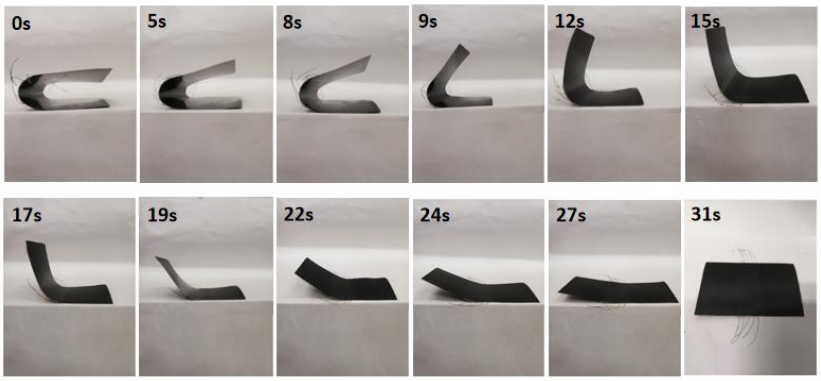

Fig. 9 Shape recovery process of the electrically-driven folding plate

Fig. 10 shows the evolution of the shape recovery angle of the electrically driven folding plate with time.

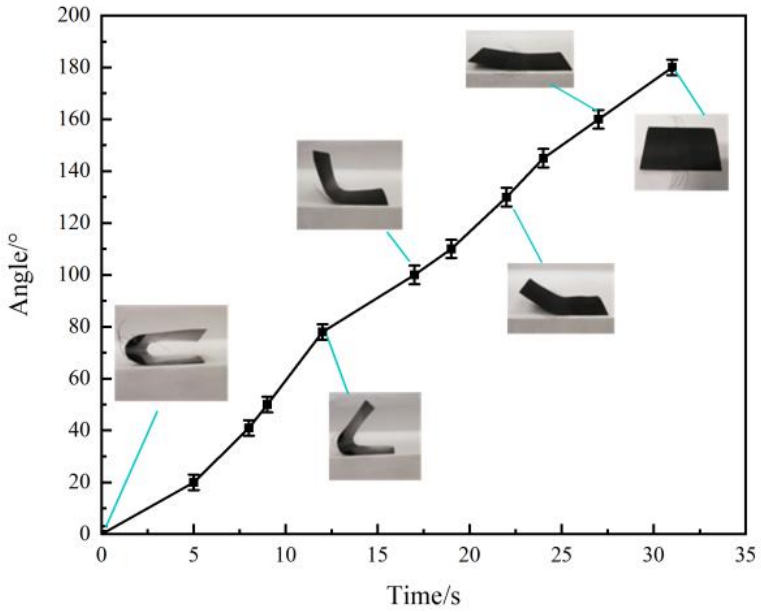

Fig. 10 Relationship between shape recovery angle and time for the electrically-driven folding plate

Under a constant current, recovery of the deformed laminate began after approximately 5 s, and nearly full recovery (≈100% of the initial flat shape) was achieved at about 31 s. During the initial 0–8 s heating stage, the specimen was rapidly heated from room temperature to the optimal actuation temperature of

~320 °C; in this period, the recovery angle remained relatively small and the recovery rate was low, reaching only ~60°. As the temperature increased, the recovery angle continued to grow, and the recovery rate between 8 and 31 s was higher than in the other time intervals. It should also be noted that the overall recovery rate is strongly governed by the magnitude of the applied voltage and the electrical properties of the composite. Compared to conventional shape memory polymers that achieve actuation near their glass transition temperature, the high actuation temperature of 320°C imposes significant limitations on this material's application in temperature-sensitive precision devices.

3.3 Electrically driven behavior of complex structures

To further validate the applicability of electrically driven materials for practical structural deformation, a sequentially foldable deformation structure was designed and fabricated. The physical prototype and dimensional schematic are shown in Fig. 11. To enable more precise temperature regulation, a 9 μm-thick copper foil layer was added to the outermost surface of the specimen as a thermal conduction layer. Together, the Ni–Ti alloy wires and copper foil form the conductive layer. The copper foil primarily serves to redistribute the heat generated by the energized alloy wires more uniformly across the composite surface, thereby ensuring more homogeneous heating.

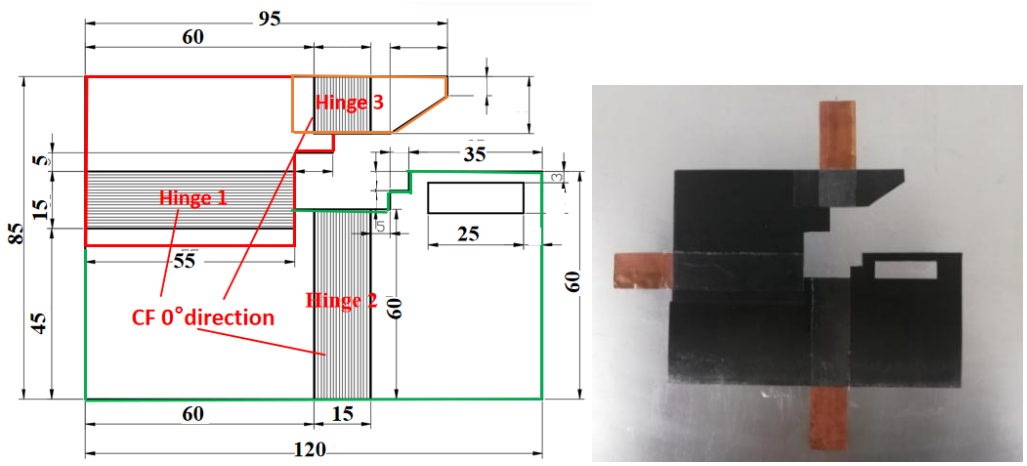

(a) Dimensional design schematic (b) Physical prototype

Fig. 11 Dimensional schematic and physical photograph of the active deformation structure in the shape memory composite (mm)

On the basis of preliminary experiments, deformation of the specimen was found to occur along the 90° fiber direction. To avoid constraining the active deformation of the hinges, a layered configuration using a spliced layup was therefore adopted during fabrication. The regions marked in green, red, and orange

indicate the seam locations and edge dimensions of the specimen. By employing a staggered layup, the seams were placed in non-deformation zones so that they did not interfere with deformation in the active regions. Subsequently, the hinge layup was introduced at the designated locations. The layup procedure followed the method described above, after which hot-press molding was carried out to ensure proper curing and integration of all structural layers with the spliced regions. In this way, the specimen was able to achieve the desired deformation while maintaining adequate stiffness and mechanical performance. Hinge 1 has dimensions of 55 mm × 15 mm × 0.15 mm, Hinge 2 measures 50 mm × 15 mm × 0.15 mm, and Hinge 3 measures 15 mm × 15 mm × 0.15 mm.

Careful attention was given to the dimensions of the locking region. A 5 mm positioning clearance was reserved at the contact interface between Hinge 1 and the green region. This design concentrates the bending deformation of Hinge 1 near its center, ensuring the effective folded height of the red region and preventing height mismatch between the locking zone and the rectangular opening in the green region. Similarly, a 5 mm positioning clearance was reserved at the contact interface between Hinge 3 and the red region. In addition, a 10 mm clearance was reserved beneath these regions to allow accurate alignment between the red and green areas after deformation of Hinges 1 and 2; otherwise, engagement between Hinge 3 and the rectangular opening could be compromised. Sufficient length was also reserved for the orange region containing Hinge 3. If this length were inadequate, incomplete deformation could lead to interference between the green region and the orange locking zone during deformation of Hinge 2, preventing full deployment. The detailed dimensional specifications are shown in Fig. 11(a). After the dimensional design was finalized, hot-press molding was performed, and the resulting prototype is presented in Fig. 11(b).

An electro-driven deformation experiment was subsequently performed on the specimen, and the active deformation sequence is illustrated in Fig. 12. The initial configuration is shown in Fig. 12(a). Electrical leads were attached, and the hinges were individually heated under a driving voltage of 6 V. After the external power supply was switched off, the specimen was allowed to cool, and its autonomous deformation during cooling was used to achieve a 90° folded and locked structural configuration. Hinge 1 was actuated first; after approximately 8 s, the specimen temperature reached 320 °C. The voltage was then removed, and the specimen was cooled to room temperature within about 3 s, completing the 90° cooling-induced deformation. After the deformation of Hinge 2 was completed, Hinge 3 was actuated in the same manner. The structure was thereby shown to achieve the intended locking effect, as presented in Fig. 12(b–d).

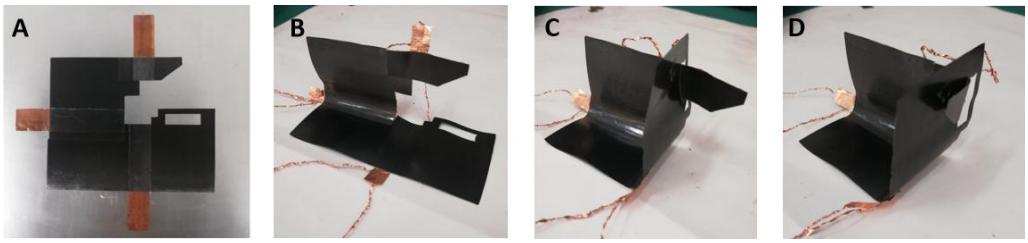

Fig.12 Active deformation process of the electrically-driven shape memory composite
(a) Undeformed state; (b)-(d) Deformed states after heating different hinges under electrically driven conditions at 6V voltage and 3.6A current

4. Conclusion

(1) For the electro-driven CF/PEEK composite lamellar hinge, nearly complete recovery to the original shape is achieved within 13 s under a 6 V electric field. The relationship between recovery angle and time shows that angular recovery is slow during the initial 0–5 s. The specimen temperature rises to approximately 320 °C within about 8 s, after which the recovery rate increases markedly.

(2) Under purely thermal actuation, the lamellar hinge attains full recovery in approximately 20 s, but the surface temperature remained nonuniform throughout the unfolding process. In contrast, electro-driven actuation yields 100% recovery within a shorter time of about 13 s. After heating and removal of the external load, the electro-driven specimen also exhibits superior stability in the fixed shape.

(3) When driven by a 6 V DC circuit, the shape memory folding plate recovers from a 180° folded configuration to a fully unfolded planar state within approximately 31 s. Moreover, by integrating electro-driven actuation with sequential folding of a complex structure, a self-deploying folding system with an inherent locking function is successfully realized. The operating temperature of 320°C for this material represents the primary limitation in its current applications. Its engineering use is thus far largely confined to self-deploying structures with low thermal load requirements and without stringent temperature control needs.

(4) In the engineering applications of CF/PEEK composite foldable hinges, safety and reliability are paramount considerations. This hinge system employs a 6V safety low-voltage drive, with the conductive layer insulated and protected by a PEEK coating. For applications near the human body, an additional polyimide thermal insulation layer can be incorporated to further enhance thermal safety. To reduce mechanical wear and extend service life, applying a PTFE coating to friction interfaces is recommended. For extreme conditions like aerospace applications, systematic thermal cycling and vibration testing must be conducted to comprehensively validate environmental adaptability and long-term operational reliability.

REFERENCES

[1] *Yue, X.K., Zhu, M.Z., Geng, H.H., Gong, L.J., Wang, Y.Y.,* Origami metamaterials and their applications and prospects in aerospace field. Acta Aeronautica et Astronautica Sinica, vol. 46, no. 06, pp. 260-293,2025.

[2] *Gu, J., Sun, X., Li, Z., Ruan, S., & Shen, C.,* Elastohydrodynamic lubrication analysis of polymer-on-polymer artificial hip joint of CF/PEEK composite. Journal of Applied Polymer Science, vol. 138, no. 39, pp. 50996, 2021. https://doi.org/10.1002/app.50996

[3] *Zhang, M.L., Yue, W.B., Lang, X.Z., Wang, X.J., Yang, J.,* Development and Application of Special Engineering Plastics: Semi- aromatic Polyamide. China Plastics, vol. 34, no. 5, pp. 115-122, 2020. DOI: 10.19491/j.issn.1001-9278.2020.05.018

[4] *Kumar, S., Ojha, N., Ramesh, M. R., & Doddamani, M.,* 4D printing of heat-stimulated shape memory polymer composite for high-temperature smart structures/actuators applications. Polymer Composites, vol. 45, no. 17, pp. 15460-15490, 2024. https://doi.org/10.1002/pc.28844

[5] *Yan, S., Zhang, F., Luo, L., Wang, L., Liu, Y., & Leng, J.,* Shape memory polymer composites: 4D printing, smart structures, and applications. Research, vol. 6, pp. 0234, 2023. DOI: 10.34133/research.0234

[6] *Aberoumand, M., Rahmatabadi, D., Soltanmohammadi, K., Soleyman, E., Ghasemi, I., Baniassadi, M., Baghani, M.,* Stress recovery and stress relaxation behaviors of PVC 4D printed by FDM technology for high-performance actuation applications. Sensors and Actuators A: Physical, vol. 361, pp. 114572, 2023. https://doi.org/10.1016/j.sna.2023.114572

[7] *Tang, D., Zhang, L., Zhang, X., Xu, L., Li, K., & Zhang, A.,* Bio-mimetic actuators of a photothermal-responsive vitrimer liquid crystal elastomer with robust, self-healing, shape memory, and reconfigurable properties. ACS Applied Materials & Interfaces, vol. 14, no. 1, pp. 1929-1939, 2021. https://doi.org/10.1021/acsami.1c19595

[8] *Yang, Y., Terentjev, E. M., Wei, Y., & Ji, Y.,* Solvent-assisted programming of flat polymer sheets into reconfigurable and self-healing 3D structures. Nature Communications, vol. 9, no. 1, pp. 1906, 2018. https://doi.org/10.1038/s41467-018-04257-x

[9] *Ma, X.Q., Zong, W.B., Zhang, Z.Q., Jiang, L., Sang, L., Wu, H.H.,* Preparation and research of ultra-thin thermoplastic composite TRAC boom. Composites Science and Engineering, no. 07, pp. 65-71, 2023. DOI: 10.19936/j.cnki.2096-8000.20230728.009

[10] *Wang, Z.Q., Zhou, X.Y., Zhu, N., Xu, C.Y., Chen, H.R.,* Research progress of thin-walled deformable carbonfiber composites in spacecraft. Fiber Composites, vol. 42, no. 04, pp. 69-78, 2025.

[11] *Zhu, S.J., Zhang, J.N., Wang, C.Y., Yang, X.T., Wang, P., Guo, H.W., Wu, H.H., Tong, L.Y.,* Shape memory effect of carbon fibers reinforced PEEK composite. Acta Materiae Compositae Sinica, vol. 38, no. 9, pp. 2832-2840, 2021. DOI: 10.13801/j.cnki.fhclxb.20201229.001

[12] *Zhao, Y., Sun, M.C., Zhang, S.Y., Wang, K.,* Advance in continuous carbon fiber reinforced high performance thermoplastic composites. Acta Materiae Compositae Sinica, vol. 39, no. 09, pp. 4274-4285, 2022. DOI: 10.13801/j.cnki.fhclxb.20220809.008

[13] *Jiang, J.H., Shao, H.Q., Chen, N.L.,* Advances in Research of Warp-knitted Reinforced Composites. China Textile Leader, no. 05, pp. 28-35, 2022. DOI: 10.16481/j.cnki.ctl.2022.05.006

[14] *Zhou, X.T., Wang, D., Ma, X.F.,*A Review of Modeling Analysis of Shell Membrane Structures in Spatially Expandable Structures. Space Electronic Technology, vol. 16, no. 3, pp. 15-25, 2019.

[15] *Ren, T.N., Zhu, G.M., Nie, J.,* Research Progress on Deployable Structures of Shape Memory Polymer Composites. Journal of Aeronautical Materials, vol. 38, no. 4, pp. 47-55, 2018.

[16] *Zong, X.J., Jiao, Y.N., Yang, X.Y., He, Y.M., Chen, L.,* Folding properties of carbon fiber triaxial woven fabric/epoxy resin composites. Acta Materiae Compositae Sinica, vol. 40, no. 06, pp. 3270-3278, 2023. DOI: 10.13801/j.cnki.fhclxb.20220907.003

[17] *Dai, G., Zhan, L., Guan, C., & Huang, M.,* The effect of moulding process parameters on interlaminar properties of CF/PEEK composite laminates. High Performance Polymers, vol. 32, no. 7, pp. 835-841, 2020.

[18] *Meng, H., & Li, G.,* A review of stimuli-responsive shape memory polymer composites. Polymer, vol. 54, no. 9, pp. 2199-2221, 2013. https://doi.org/10.1016/j.polymer.2013.02.023

[19] *Wang, Y.L., Sha, Z.D., She, C.M.,* Research on mechanical properties of the deployable structure with adjustable thermal expansion coefficient. Chinese Journal of Theoretical and Applied Mechanics, vol. 57, no. 03, pp. 701-711, 2025. DOI: 10.6052/0459-1879-24-429

[20] *Zhang, Z., Li, S.C., Zhang, J.N., Wang, C.Y., Ba, W.L., Wu, H.H.,* Effect of ultra-thinning of prepreg on tensile failure behavior of carbon fiber/epoxy resin composites. Acta Materiae Compositae Sinica, vol. 37, no. 4, pp. 800-807, 2020. DOI: 10.13801/j.cnki.fhclxb.20190628.001